

See discussions, stats, and author profiles for this publication at: <https://www.researchgate.net/publication/45404868>

Multicomponent Hollow Tubules Formed Using Phytosterol and γ -Oryzanol-Based Compounds: An Understanding of Their Molecular Embrace

ARTICLE *in* THE JOURNAL OF PHYSICAL CHEMISTRY A · AUGUST 2010

Impact Factor: 2.69 · DOI: 10.1021/jp104101k · Source: PubMed

CITATIONS

21

READS

39

5 AUTHORS, INCLUDING:



[Michael A Rogers](#)

University of Guelph

65 PUBLICATIONS 1,058 CITATIONS

[SEE PROFILE](#)



[Arjen Bot](#)

Unilever

79 PUBLICATIONS 1,356 CITATIONS

[SEE PROFILE](#)



[Ricky Sze Ho Lam](#)

University of Saskatchewan

15 PUBLICATIONS 172 CITATIONS

[SEE PROFILE](#)



[Tim May](#)

Canadian Light Source Inc. (CLS)

39 PUBLICATIONS 221 CITATIONS

[SEE PROFILE](#)

Multicomponent Hollow Tubules Formed Using Phytosterol and γ -Oryzanol-Based Compounds: An Understanding of Their Molecular Embrace

Michael A. Rogers,^{*,†} Arjen Bot,[‡] Ricky Sze Ho Lam,[†] Tor Pedersen,[§] and Tim May[§]

Department of Food and Bioproduct Sciences, University of Saskatchewan, Saskatoon, SK, Canada, S7N5A8, Unilever Research and Development Vlaardingen, Olivier van Noortlaan 120, NL-3133 AT Vlaardingen, The Netherlands, and Canadian Light Source, Saskatoon, SK, S7N0X4, Canada

Received: May 5, 2010; Revised Manuscript Received: July 1, 2010

The formation kinetics of self-assembling tubules composed of phytosterol: γ -oryzanol mixtures were investigated at the Canadian Light Source on the mid-IR beamline using synchrotron radiation and Fourier transform infrared spectroscopy (FT-IR). The Avrami model was fitted to the changing hydrogen bonding density occurring at 3450 cm^{-1} . The nucleation process was found to be highly dependent on the molecular structure of the phytosterol. The nucleation event for cholesterol: γ -oryzanol was determined to be sporadic whereas 5α -cholestane- 3β -ol: γ -oryzanol and β -sitosterol: γ -oryzanol underwent instantaneous nucleation. One-dimensional growth occurred for each phytosterol: γ -oryzanol mixture and involved the evolution of highly specific intermolecular hydrogen bonds. More detailed studies on the cholesterol: γ -oryzanol system indicated that the nucleation activation energy, determined from multiple rate constants, obtained using the Avrami model, was at a minimum when the two compounds were at a 1:1 weight ratio. This resulted in drastic differences to the microscopic structures and affected the macroscopic properties such as turbidity. The formation of the phytosterol: γ -oryzanol complex was due to intermolecular hydrogen bonding, which was in agreement with the infrared spectroscopic evidence.

Introduction

Molecularly self-assembled one-dimensional nanostructures have numerous potential applications including medical applications, chemical synthesis, external pressure responsive systems, and electronics. Self-assembly into one-dimensional fibers exhibit distinct features whereby the assembling molecules, within the cross-section of the fiber are highly ordered, similar to crystalline materials.¹ However, along the fiber axis, disorder may be incorporated, resulting in crystallographic mismatches causing the fiber to branch.¹ Self-assembly has been an area of active research attempting to acquire a fundamental knowledge which focuses on supramolecular chemistry and on gaining an understanding of the tailorability of physical parameters including size, shape, and external and internal structures.² However, the process of self-assembly still has a plethora of unanswered questions such as “why” and “how” do these materials assemble into fibrillar networks.³

Molecular self-assembly may occur either spontaneously or under the influence of external forces such as shear,⁴ pH,⁵ temperature,⁶ light,⁷ or electric fields.⁸ By varying the magnitude of these external forces, it is possible to control the size, dimensionality of growth, and the spatial distribution of mass. In many instances, molecular self-assembly occurs via a supersaturated state whereby the “gelator”—solvent melt is cooled below the melting point of the gelator, triggering the gelator to microscopically phase-separate and self-assemble via stochastic nucleation events driven by enthalpic forces.⁹ Depending on the degree of supercooling, nucleation may occur either sporadically or instantaneously

and is then followed by crystal growth causing gelator to accrete on the surface of the stable nuclei forming fibers via highly specific noncovalent interactions. The process of one-dimensional growth requires a meticulous balance between the contrasting parameters of solubility and those which control epitaxial growth, leading to an elongated axis.¹⁰ This unique one-dimensional supramolecular configuration presents useful properties such as alignment, conductivity, biological interactions, and templating of novel soft materials.² In specific cases, the supramolecular assemblies may form organogels which aggregate to form three-dimensional networks entrapping the solvent phase.

Considerable attention has recently focused on the ability of γ -oryzanol and different phytosterols to form hollow tubules of 7 nm diameter and just under 1 nm wall thickness.^{11–15} Mixtures of phytosterol and γ -oryzanol establish a continuous three-dimensional network of hollow tubules capable of immobilizing apolar solvents such as polyunsaturated triglyceride oils over macroscopic length scales.^{11,12,14} The tubule formation is a synergistic phenomenon between the phytosterol and the γ -oryzanol, because individually neither are capable of entrapping the oil phase.¹¹ Previous research also demonstrated that β -sitosterol-rich organogels tend to be more turbid, which was attributed to enhanced aggregation of the tubules, leading to larger junction zones in the organogel since the diameter of the tubule does not change as a function of phytosterol: γ -oryzanol ratio.¹² At a 8:8 wt %/wt% ratio, these compounds produce a transparent gel.¹² While acknowledging the many regulatory restrictions on applications in foods, cosmetics, and medicine, we envisage numerous potential applications of these tubules, such as drug carriers for transdermal applications, encapsulation of nutraceuticals, and perhaps most intriguing a trans-saturated fat replacer. The use of the γ -oryzanol:phytosterol mixtures for hardstock replacement is interesting because it circumvents the need for trans or saturated fats, normally required to structure edible oils as a colloidal dispersion which provides

* Corresponding author: E-mail: michael.rogers@usask.ca. Tel: + 306 966 5028. Fax: + 306 966-8898.

[†] University of Saskatchewan.

[‡] Unilever Research and Development Vlaardingen.

[§] Canadian Light Source.

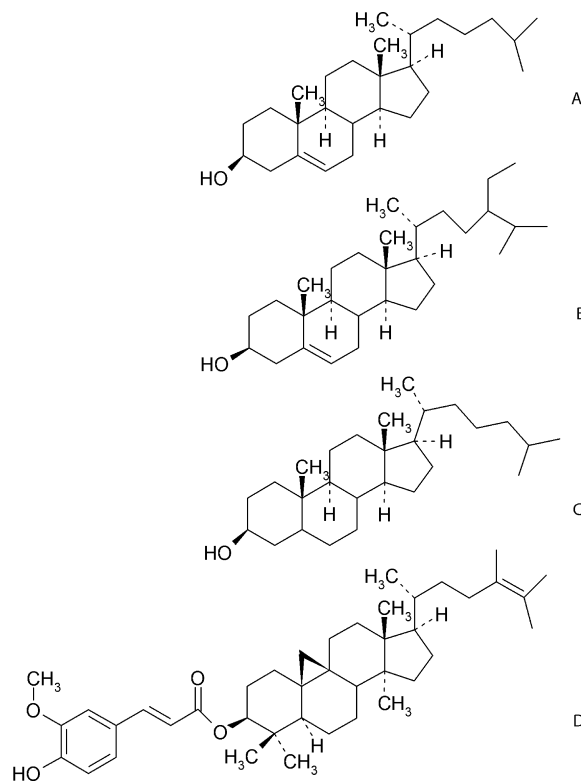


Figure 1. Chemical structures for cholesterol (A), β -sitosterol (B), 5α -cholestane- 3β -ol (C), and γ -oryzanol (D).

the desirable elastic properties of soft materials. Further, trans and saturated fats have been associated with numerous physiological phenomena including adverse effects on lipoprotein (cholesterol) profiles.¹⁶ The negative health implications associated with consuming trans and saturated fats may be reversed by reducing the intake of these heart-unhealthy fats or replacing them with polyunsaturated fats.¹⁷

Limited knowledge is available on the kinetics of self-assembly in these multicomponent systems, and the present study serves as a means to fill this knowledge gap. More specifically, it has been observed that the phytosterol: γ -oryzanol systems can be supercooled relatively easily,¹¹ suggesting a nucleation-growth type process. The aim of this study was to physically characterize the phytosterol: γ -oryzanol systems and to determine the basic parameters of the self-assembly process. This was achieved by monitoring the concentration of intermolecular hydrogen bonding required for tubule formation in these systems by means of FT-IR spectroscopy.

Methods

Cholesterol and 5α -cholestane- 3β -ol were both acquired from Sigma-Aldrich (Oakville, ON, Canada), β -sitosterol was obtained from Acros Organics (Geel, Belgium), and γ -oryzanol was obtained from Tsuno Rice Fine Chemicals (Wakayama, Japan) (Figure 1). Each was dispersed in heavy mineral oil obtained from Sigma-Aldrich (Oakville, ON, CAN) and not purified further. γ -Oryzanol is a mixture of 45.9% 24-methenecycloartenyl ferulate, 26.8% cycloartenyl ferulate, 13.1% campesteryl ferulate, 7.1% sitosteryl ferulate, 1.4% δ^5 -avenasteryl ferulate, 1.3% stigmasteryl ferulate, 1.0% campestanol ferulate (Tsuno Rice Fine Chemicals Co, Wakayama, Japan). Samples of cholesterol were prepared with varying concentrations in mineral oil and heated to 120 °C for 30 min, and a drop of molten sample was placed between two CaF_2 optical windows (25 mm diameter, 2 mm thick) separated with a

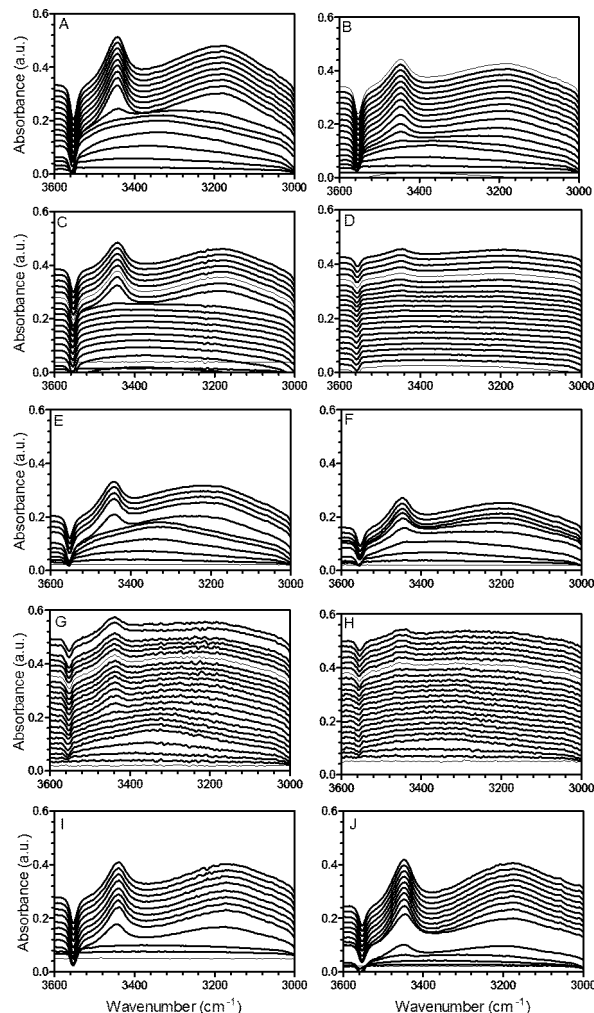


Figure 2. Changing FT-IR signal for 8:8 wt%:wt% cholesterol: γ -oryzanol at 10 °C (A) and 40 °C (B); 8:4 wt%:wt% cholesterol: γ -oryzanol at 10 °C (C) and 40 °C (D); 8:12 wt%:wt% cholesterol: γ -oryzanol at 10 °C (E) and 40 °C (F); 4:8 wt%:wt% cholesterol: γ -oryzanol at 10 °C (G) and 40 °C (H); 12:8 wt%:wt% cholesterol: γ -oryzanol at 10 °C (I) and 40 °C (J). The time between displayed spectra is 1 min.

15 μm Teflon spacer. The samples were transferred onto a Linkam LTS120 controlled temperature stage (Linkam, Surrey, United Kingdom) and were isothermally cooled to 10, 20, 30, and 40 °C. In a manner similar to that previously mentioned, 8:8 wt%:wt% cholesterol: γ -oryzanol, 8:8 wt%:wt% 5α -cholestane- 3β -ol: γ -oryzanol, and 8:8 wt%:wt% β -sitosterol: γ -oryzanol mixtures were prepared.

Fourier transform infrared (FT-IR) spectra were collected using the end station of the mid-IR beamline (beamline 01B1-01, Canadian Light Source, Saskatoon, SK). The end station is composed of a Bruker Optics IFS66v/S interferometer coupled to a Hyperion 2000 IR microscope (Bruker Optics, Billerica, MA). Light was focused on the sample using a 15 \times magnification Schwarzschild condenser, collected by a 15 \times magnification Schwarzschild objective with the aperture set to a spot size of 40 μm by 40 μm and detected by a liquid nitrogen-cooled narrowband MCT detector utilizing a 100 μm sensing element.

A KBr-supported Ge multilayer beamsplitter was used to measure spectra in the mid-infrared spectral region. Measurements were performed using OPUS 6.5 software (Bruker Optics). The measured interferograms were an average of 32 scans and were recorded by scanning the moving mirror at 40 kHz (in relation to the reference HeNe laser wavelength of 632.8 nm). Scans were taken every 10 s. The wavelength range collected was 690 to 7899

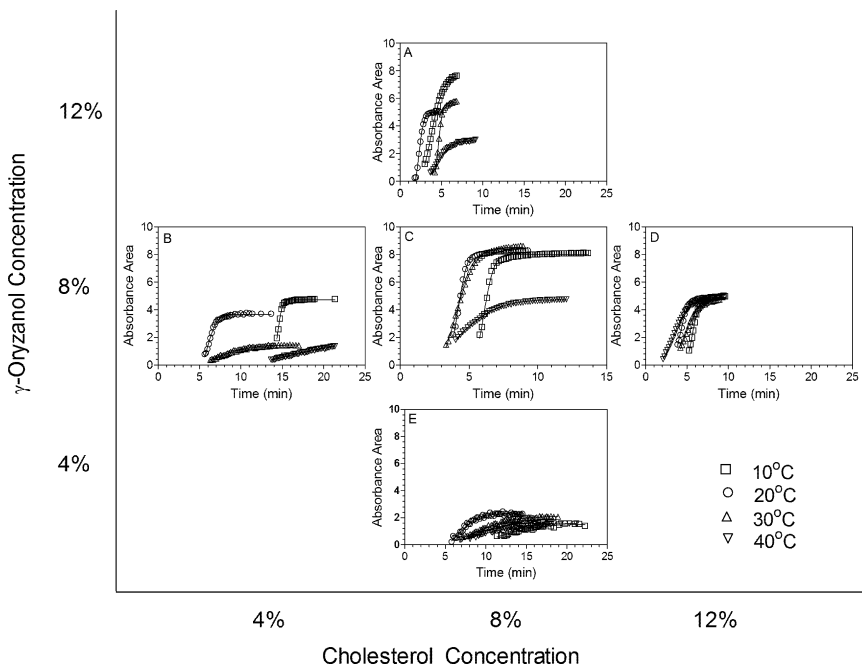


Figure 3. Integration of the FT-IR signal at 3450 cm^{-1} for 12:8 wt %:wt% cholesterol: γ -oryzanol (A); 8:4 wt %:wt% cholesterol: γ -oryzanol (B); 8:8 wt %:wt% cholesterol: γ -oryzanol (C); 8:12 wt %:wt% cholesterol: γ -oryzanol (D); and 4:8 wt %:wt% cholesterol: γ -oryzanol (E).

cm^{-1} with a spectral resolution of 4 cm^{-1} . Single channel traces were obtained using the fast Fourier transform algorithm, without any zero-filling, after applying a Blackman-Harris 3-Term apodization function. For single spectra measurements, reference single channel traces were carried out in the molten state.

Polarized light micrographs were acquired using a Nikon Eclipse E400 light microscope equipped with a Nikon DS-FiL color camera and a long working distance $10\times$ lens and condenser with a resolution of 2560 by 1920. Samples were cooled at $1\text{ }^{\circ}\text{C}/\text{min}$ to $30\text{ }^{\circ}\text{C}$ using a temperature-controlled stage (LTS 120 and PE94 temperature controller (Linkam, Surrey, United Kingdom).

Turbidity was determined using a Genesys 10uv spectrophotometer (Thermo Scientific, Asheville, NC) using a wavelength of 800 nm . A 800 nm wavelength was chosen because it is within the Herschel near infrared range ($700\text{--}1100\text{ nm}$). Because three-dimensional solids exhibit absorbance at virtually all frequencies of light, in the NIR region, solids contributing to turbidity can be isolated from visible color and other dissolved constituents.

Ten to twelve milligrams of 8:8 wt % phytosterol: γ -oryzanol in mineral oil was placed in Alod-Al hermetic DSC pans and heated to $120\text{ }^{\circ}\text{C}$ and then was subsequently cooled at $10\text{ }^{\circ}\text{C}/\text{min}$ to $10\text{ }^{\circ}\text{C}$ and held for 10 min using a Q2000 differential scanning calorimeter (DSC) (TA Instruments, New Castle, DE). Following the holding period, the samples were heated to $120\text{ }^{\circ}\text{C}$ at $10\text{ }^{\circ}\text{C}/\text{min}$ and the melting temperature was recorded while the chamber was continually flushed with nitrogen ($0.5\text{ mL}/\text{min}$). Each run was performed in triplicate.

Results and Discussion

The effect of different weight ratios for the phytosterol (i.e., cholesterol) and γ -oryzanol, in heavy mineral oil, on the kinetics of tubule formation was examined using the change in the FT-IR spectrum area between 3000 and 3600 cm^{-1} , as a function of time (Figure 2). The change in the FT-IR spectrum area wavenumber range between 3200 and 3600 cm^{-1} is used to monitor nonspecific hydrogen bonding for alcohols and phenols.¹⁸ It is evident from

Figure 2 that as the sample is cooled, the cholesterol: γ -oryzanol system develops nonspecific hydrogen bonding which is observed by the evolution of a weak, broad peak from 3600 to 3200 cm^{-1} corresponding to a decrease in the free hydroxyl stretch at 3600 cm^{-1} . This nonspecific peak may exist at upward of 10 min before the evolution of the highly specific interactions between cholesterol and γ -oryzanol resulting in a sharp absorbance around 3450 cm^{-1} . This may suggest the formation of a metastable state or the formation of a crystal containing pure cholesterol or γ -oryzanol prior to the formation of the multicomponent tubular structures. Once a sufficient quantity of the excess compound has crystallized out, the appropriate ratio may exist between the cholesterol and γ -oryzanol, resulting in a new crystal morphology which consists primarily of tubules. Further, it is evident that this nonspecific region of interest exists for a longer period of time when it is gelled at $40\text{ }^{\circ}\text{C}$ (Figure 2B,D,F,H,J) compared to $10\text{ }^{\circ}\text{C}$ (Figure 2A,C,E,-G,I). From Figure 2 it is observed that the tubule formation relies on highly specific intermolecular hydrogen bonding between the hydroxyl groups on γ -oryzanol and cholesterol, as demonstrated by the presence of a sharp peak at 3450 cm^{-1} . This peak is positioned within the range of wavenumbers associated with hydroxyl hydrogen bonding. Further, the generation of hydrogen bonding between hydroxyl groups (i.e., peak seen at 3450 cm^{-1}) further supports the simultaneous decrease in the absorbance at approximately 3600 cm^{-1} , corresponding to the decreasing concentration of free hydroxyl groups.¹⁸ Therefore, the existence of the peak observed at 3450 cm^{-1} is attributed to intermolecular hydrogen bonding corresponding to a depletion of free hydroxyl groups.¹⁹ Further to this argument, the mineral oil only contributes to CH_2 and CH_3 stretches and these do not interfere with the spectral regions of interest. The only other spectral features present in this system can be attributed to the carbonyl and ester groups on γ -oryzanol which do not have spectral features above 1700 cm^{-1} and 1750 cm^{-1} , respectively.¹⁸ Since the self-assembly process of these compounds may be monitored through a quantitative assessment of the peak area at 3450 cm^{-1} (Figure 2), this area was measured and the rate of hydrogen bonding increase during crystallization was determined (Figure 3). The change in the area

TABLE 1: *n*-Values Determined for Different Ratios of γ -Oryzanol and Cholesterol Using the Avrami Model Fitted to the Changing Area at 3450 cm^{-1} Using FT-IR under Isothermal Crystallization Conditions^a

γ -oryzanol:cholesterol ratio	<i>n</i> -value
8:12	2.12 ± 0.12
8:8	2.12 ± 0.36
8:4	1.88 ± 0.35
12:8	2.00 ± 0.35
4:8	2.15 ± 0.30

^a *n* is an average of each fit at the different isothermal temperatures. There is no statistical ($P < 0.05$) difference between samples at each ratio level.

of the hydrogen bonding for the hydroxyl groups demonstrates the typical sigmoidal shaped growth curve. The crystallization process starts slowly, followed by a steady-state region and ends in a slow evolution of crystal growth. Figure 3 indicates that as the isothermal driving force for crystallization decreases (i.e., higher crystallization temperatures), the amount of crystalline material and the rate of crystallization decrease.

H-bonding between hydroxyl and carboxyl acid groups for nanofibers of 12-hydroxystearic acid have previously been fitted to a modified Avrami model developed for nonisothermal cooling conditions to determine the rate constant as well as the dimensionality of crystal growth.^{6,20–22} The current experimental design utilizes isothermal cooling conditions, allowing the Avrami model to be fitted to the changing area of the peak at position 3450 cm^{-1} :

where Y is a relative measure of the crystalline material or the area of the FT-IR signal at 3450 cm^{-1} , K is the rate constant of growth, t is the time, and n is the Avrami exponent.^{22–24} The Avrami model accounts for both the change in crystallizing mass during nucleation as well as the dimensionality of crystal growth. For the data to be fitted to the phase transition, the assembly process must follow certain assumptions including the following: the cooling parameters must be isothermal; nucleation must be a spatially random event and must follow linear growth kinetics in which the growth rate of the new phase depends only on temperature and not on time.²⁵ The dimensionality of growth, n , is a function of not only the dimensionality of crystal growth but also on the mode of nucleation.²⁵ n should be a value between 1 and 4. If $n = 1$, then instantaneous nucleation and 1-D crystal growth occurs; if $n = 2$ then either instantaneous nucleation and 2-D growth occurs or sporadic nucleation with 1-D growth occurs.²⁵ Fitting our hydrogen bonding area versus time with the Avrami model for all cholesterol: γ -oryzanol ratios reveals that the dimensionality of growth is 2 (Table 1). *n* values were compared using an one way ANOVA analysis and a Tukey's multiple comparison test, and no statistical differences ($P < 0.05$) were observed between *n* values for the ratios of cholesterol and γ -oryzanol. Previous work using small-angle X-ray scattering has indicated that these mixtures form 1-D hollow fibers.^{12,13} Therefore, our work has confirmed the presence of fibers which are formed under sporadic nucleation. Since each isothermal temperature gives rise to an *n* value of 2, in

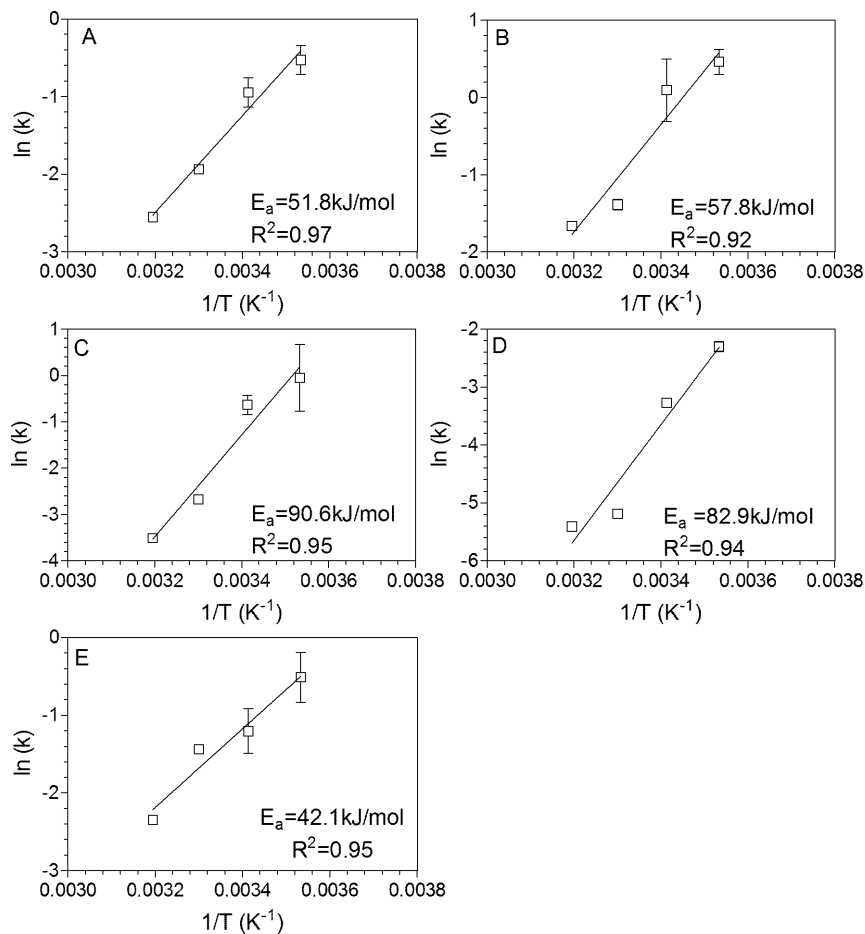


Figure 4. Determination of the activation energy from the rate constants determined using the Avrami model under isothermal crystallization conditions for 8:12 wt %:wt% cholesterol: γ -oryzanol (A), 12:8 wt %:wt% cholesterol: γ -oryzanol (B), 8:4 wt %:wt% cholesterol: γ -oryzanol (C), 4:8 wt %:wt% cholesterol: γ -oryzanol (D), and 8:8 wt %:wt% cholesterol: γ -oryzanol (E). Error bars represent the standard error.

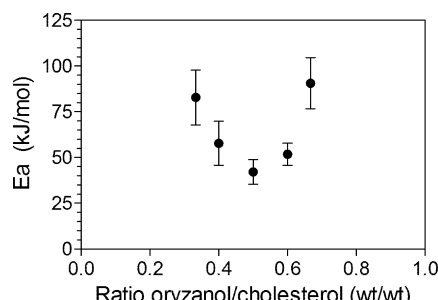


Figure 5. Activation energy (E_a) determined from the rate constants using the Avrami model as a function of the wt% / wt% ratio of γ -oryzanol:cholesterol. Error bars represent the standard error.

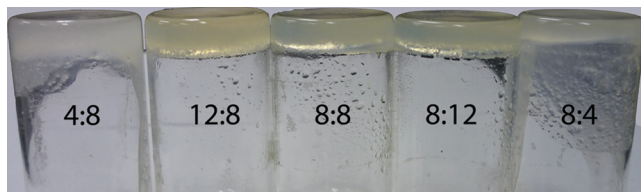


Figure 6. Photographs of the different ratios of cholesterol: γ -oryzanol quenched and cooled to 30 °C.

all instances, the rate constants (K) can be utilized from the Avrami fits to determine the activation energy of crystallization (Figure 4) via the following equation:

$$\ln K = \ln A + \frac{E_a}{RT}$$

where K is the rate constant from the Avrami fit, $\ln A$ is the y -intercept, E_a is the activation energy, R is the ideal gas constant, and T is the temperature. It is important to note that the activation energy may only be calculated if the dimensionality of growth, n , is the same at each isothermal temperature.²⁵ From Figure 5 it is apparent that the activation energy of nucleation is much higher when either cholesterol or γ -oryzanol is in a higher concentration than the other. At 8:8 wt %:wt% or a 60:40 mol:mol ratio, a transparent organogel (ABS = 0.76 ± 0.05) (Figure 6) forms, and as one of the components becomes in excess, the turbidity along with the activation energy increases. The absorbance for the other cholesterol: γ -oryzanol ratios are 8:4 wt %:wt% ABS = 1.87 ± 0.10 , 8:12 wt %:wt% ABS = 1.05 ± 0.06 , 12:8 wt %:wt% ABS = 1.68 ± 0.11 , and 4:8 wt %:wt% ABS = 1.38 ± 0.08 .

One possible explanation for the correlation between turbidity and activation energy is that as the activation energy of nucleation increases, it becomes more difficult for stable nuclei to form. Since stable nuclei are not readily formed, less growth sites are present for the assembling molecules to adhere to, resulting in either thicker or longer tubules and thus more junction zones capable of diffracting light. If the crystals are thicker or have a different morphology, or there are more junction zones, then the turbidity increases. It has been noted previously that the optimal ratio for organogel formation appears to be a 1:1 molar ratio of the plant sterol and γ -oryzanol (approximately a 40:60 weight ratio).¹⁴ From a physical chemistry point of view, this is a very important observation because it suggests that fiber formation may be a result of a formation of a hylotrope where the solid consists of equal phytosterol and γ -oryzanol composition. Typically, azeotropic behavior arises because the molecules are capable of interacting to the same degree with the other compounds as with themselves. For a solid azeotrope or hylotrope, the miscibility of

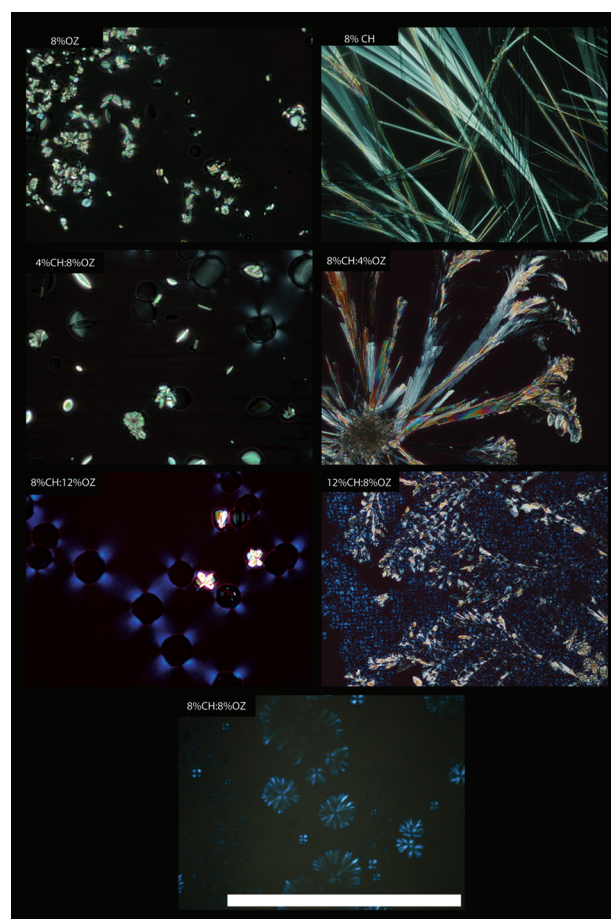


Figure 7. Polarized light micrographs of the different ratios of cholesterol (CH) and γ -oryzanol (OZ). Magnification bar = 100 μm .

the system is larger in the crystalline phase than in the corresponding melt. The activation energy of crystallization is a function of the strength of the collision required for the molecule to be incorporated into the crystal lattice but also the frequency of collisions with the proper molecular orientation. This would suggest that at a 1:1 molar ratio the frequency of collisions with the proper orientation occurs more readily than at the other ratios. Hence, for fiber formation to occur, the hydroxyl group of the cholesterol group must interact with the ester group of the γ -oryzanol, which gives rise to the 3450 cm^{-1} peak.

The individual crystal structure for 8 wt % cholesterol in mineral oil has long tubule-like fibers while that of 8 wt % γ -oryzanol in mineral oil has small plate-like crystals as depicted in Figure 7. The pure compounds form highly birefringent crystals which are capable of diffracting visible light, leading to highly turbid samples. In all samples other than 8:8 wt:wt cholesterol: γ -oryzanol, similar crystal morphologies are observed as in the individual crystal structures for either cholesterol or γ -oryzanol. However, a new crystal morphology is observed when cholesterol and γ -oryzanol are combined. The new crystal structure has fine tubules radiating from a central nucleus. In most ratios there is a presence of highly birefringent crystals as well as the new fine tubules. Only the new crystal morphology is observed at an 8:8 wt:wt ratio. The new crystal morphology may be a result of a hylotropic behavior, which results in fine tubule structures radiating from the central nucleus. This would correspond to the decrease in the overall turbidity of the gel. The change in crystal morphology (i.e., more nuclei and finer crystal growth), which is coincident with the observed decrease in the activation energy for the 8:8 wt:wt cholesterol: γ -

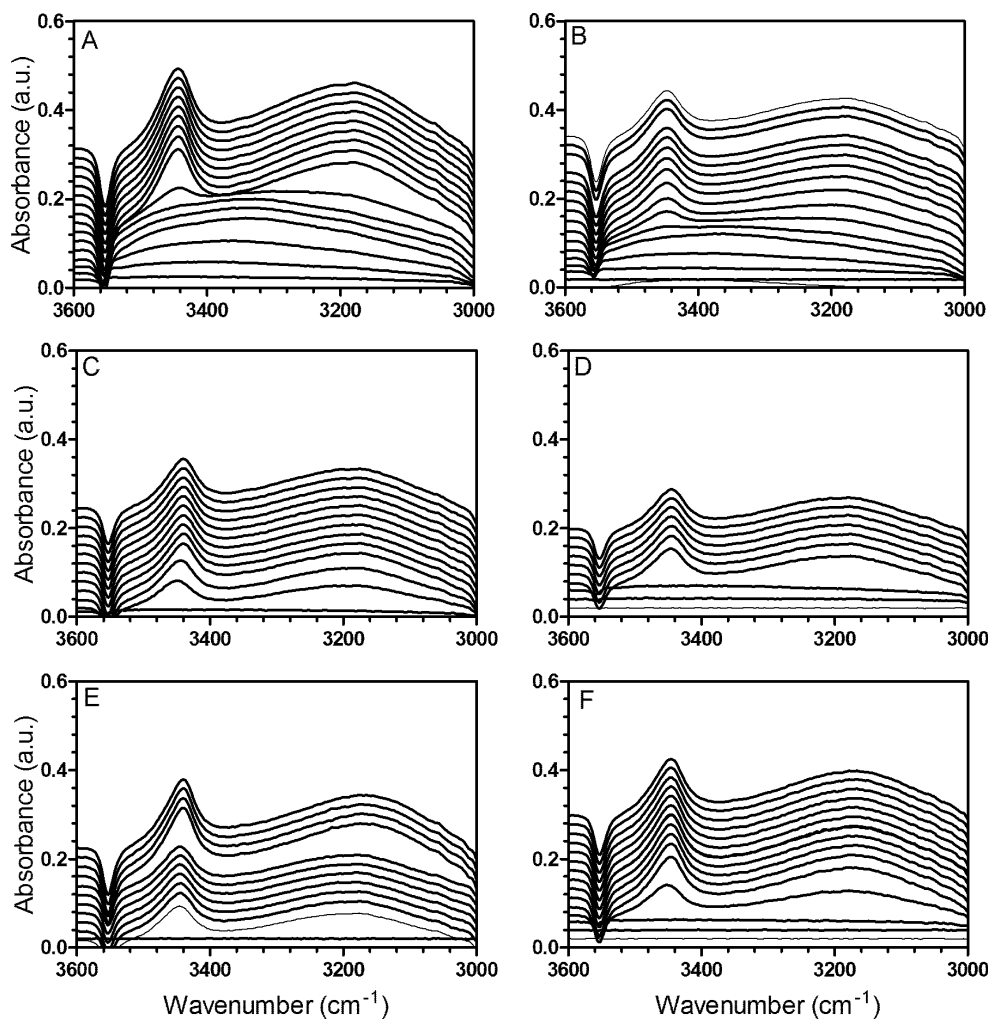


Figure 8. Changing FT-IR signal for 8:8 wt %:wt% cholesterol:γ-oryzanol at 10 °C (A) and 40 °C (B); 8:8 wt %:wt% 5α-cholestan-3β-ol:γ-oryzanol at 10 °C (C) and 40 °C (D); 8:8 wt %:wt% β-sitosterol:γ-oryzanol at 10 °C (E) and 40 °C (F). The time between displayed spectra is 1 min.

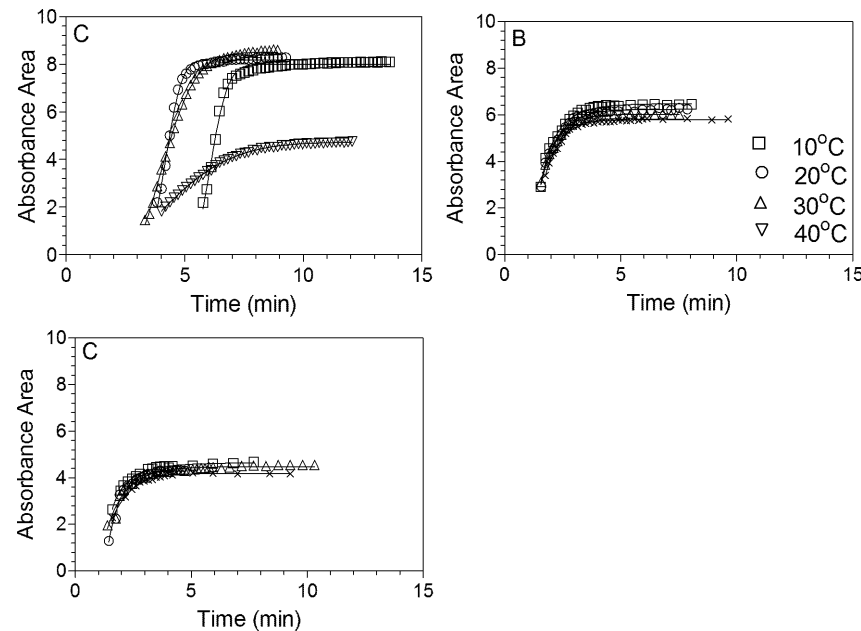


Figure 9. Integration of the FT-IR signal at 3450 cm⁻¹ for 8:8 wt %:wt% cholesterol:γ-oryzanol (A); 8:8 wt %:wt% 5α-cholestan-3β-ol:γ-oryzanol (B); 8:8 wt %:wt% β-sitosterol:γ-oryzanol (C).

oryzanol sample, results in a greater number of nuclei followed by limited crystal growth.

Early rheological data provided some information on the kinetics of assembly for different phytosterols.¹¹ A series of

TABLE 2: *n*-Values Determined for Different 8 wt % Phytosterols Mixed with 8 wt % γ -Oryzanol Using the Avrami Model Fitted to the Change Area at 3450 cm^{-1} Using FT-IR under Isothermal Crystallization Conditions^a

	<i>n</i> -value
cholesterol: γ -oryzanol	2.12 ± 0.36
5 α -cholestane-3 β -ol: γ -oryzanol	1.00 ± 0.18
β -sitosterol: γ -oryzanol	0.96 ± 0.21

^a *n* is an average of each fit at the different isothermal temperatures.

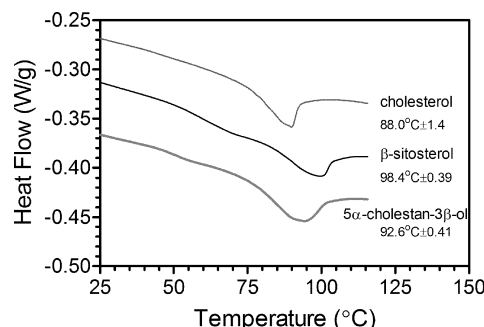


Figure 10. Differential scanning calorimetry thermograms for 8:8 wt %:wt% cholesterol: γ -oryzanol, 8:8 wt %:wt% 5 α -cholestane-3 β -ol: γ -oryzanol, and 8:8 wt %:wt% β -sitosterol: γ -oryzanol. The temperature presented for each sample is the average peak melting temperature \pm the standard deviation of three replicates. Error bars represent the standard error.

observations were deduced: a hydroxyl group on the phytosterols is essential for assembly into tubules; an absence of double bonds in the phytosterol rings increases the rate of assembly; the aliphatic side chain has a moderate effect on the occurrence of gelation.¹¹ Using the aforementioned techniques described in this paper, spectra were collected every 10 s but were plotted at every minute for illustrative purposes (Figure 8). Three phytosterols, cholesterol (Figure 8A,B), 5 α -cholestane-3 β -ol (Figure 6C,D), and β -sitosterol (Figure 8E,F), were examined. Cholesterol and 5 α -cholestane-3 β -ol differ only based on the

presence of a double bond in the ring structure while the β -sitosterol and cholesterol differ based on the alkyl side chain but both have the double bond in the ring structure (Figure 1). Cholesterol: γ -oryzanol (Figure 8A,B) shows the evolution of a broad peak from 3600 to 3200 cm^{-1} and then undergoes a molecular rearrangement which is indicated by the evolution of a sharp peak at 3450 cm^{-1} . However, for both 5 α -cholestane-3 β -ol: γ -oryzanol and β -sitosterol: γ -oryzanol, the phase transition occurs without the presence of the metastable region and the sharp peak at 3450 cm^{-1} develops directly from the melt. The area of the peak at 3450 cm^{-1} was determined and plotted as a function of time and fitted to the Avrami model (Figure 9). Upon fitting, the *n* values illustrated that cholesterol: γ -oryzanol underwent sporadic nucleation followed by 1-D growth while 5 α -cholestane-3 β -ol and β -sitosterol both underwent instantaneous nucleation followed by 1-D growth (Table 2). Sporadic nucleation generally occurs when the driving force for nucleation is low or the activation energy for nucleation is high while for instantaneous nucleation, a high driving force for nucleation or a low activation energy is observed. A tentative explanation for the difference between the cholesterol: γ -oryzanol mixture and the other two mixtures could be the lower melting temperature of the cholesterol-based mixture (88.0 ± 1.4 °C) compared to that of the cholestanol (92.6 ± 0.41 °C) and sitosterol (98.4 ± 0.39 °C) based systems (Figure 10).¹³ The closer proximity to the melting transition apparently affects the nucleation process but not the growth mechanism. The FT-IR data support the initial existence of a separate metastable state with nonspecific hydrogen bonding, as indicated by an increase in the area of the hydroxyl hydrogen bonding region between 3200 to 3600 cm^{-1} for cholesterol (Figure 8A,B). It is not until 5 min that there is a molecular rearrangement forming highly specific hydroxyl–hydroxyl interactions between cholesterol and γ -oryzanol (Figure 8A,B). 5 α -Cholestane-3 β -ol and β -sitosterol both go directly from the sol state to the highly ordered state. For these two phytosterols, the melt does not pass through the metastable region, indicated by the lack of a broad peak at 3200 to 3600 cm^{-1} (Figure 8C–F). This observation also reconfirms the different *n* values determined by the Avrami model (Table 2).

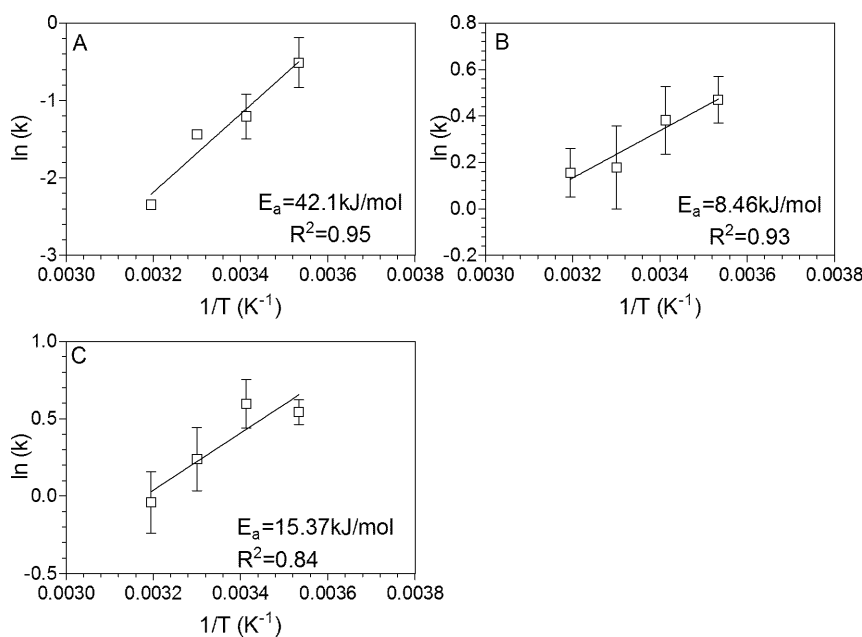


Figure 11. Determination of the activation energy from the rate constants determined using the Avrami model under isothermal crystallization conditions for 8:8 wt %:wt% cholesterol: γ -oryzanol (A), 8:8 wt %:wt% 5 α -cholestane-3 β -ol: γ -oryzanol (B), and 8:8 wt %:wt% β -sitosterol: γ -oryzanol (C). Error bars represent the standard error.

2). The activation energy for each 8:8 wt %:wt% phytosterol: γ -oryzanol sample was determined (Figure 11) and indicated that cholesterol had the highest activation energy (41.2 kJ/mol) while 5 α -cholestan-3 β -ol had the lowest activation energy (8.46 kJ/mol). The activation energy for cholesterol was considerably higher than that of the other two phytosterols and as a result exhibits a metastable region (Figure 8A,B) prior to the formation of the highly specific interactions required for fiber formation. This supports previous observations by Bot and Agterof that the fastest gelling system had no double bonds in the ring structure.¹¹ The rate of gelation is related to the ease of formation of the initial nuclei, which in turn depends on the degree of supercooling. Interestingly, however, the small variation in the aliphatic chain causes dramatic differences in both the type of nucleation and the activation energy of nucleation. β -Sitosterol has an aliphatic chain similar to that of γ -oryzanol while cholesterol does not, and this leads to an increased ease in the formation of a complex with the γ -oryzanol (Figure 1). With slight modifications to the phytosterol structure, the kinetics of the phase transition may be modified which may further lead to the tailorability of the supramolecular tubule.

Conclusion

Modifications to the ratio of phytosterol to γ -oryzanol affect not only the opacity of gels but also the activation energy of nucleation. A minimum activation energy of nucleation is observed when there is a 8:8 wt %/wt% cholesterol: γ -oryzanol which results in the formation of very fine tubules. When the amount of phytosterol is not equal to the amount of γ -oryzanol there is an increase in the activation energy resulting in the lack of stable nuclei and hence less surface area for subsequent crystal growth that results in longer and/or thicker crystals with more junction zones capable of diffracting light. Modifying phytosterol structure results in drastic changes to the kinetics of the self-assembly as well as the final physical properties of the material. The absence of a double bond in the phytosterol ring or an aliphatic chain similar to that of γ -oryzanol reduces the activation energy of crystallization while the presence of a double bond in the phytosterol ring and an aliphatic side chain different from that of γ -oryzanol increases the activation energy of nucleation resulting in sporadic nucleation.

Acknowledgment. The research described in this paper was performed at the Canadian Light Source, which is supported by NSERC, NRC, CIHR, and the University of Saskatchewan. This project was supported by the National Science and Engineering Research Council of Canada (NSERC) Discovery Program.

References and Notes

- (1) Douglas, J. F. *Langmuir* **2009**, *25*, 8386.
- (2) Palmer, L. C.; Stupp, S. I. *Acc. Chem. Res.* **2008**, *41*, 1674.
- (3) Weiss, R. G. *Langmuir* **2009**, *25*, 8369.
- (4) Li, D.; Kaner, R. B. *J. Am. Chem. Soc.* **2006**, *128*, 968.
- (5) Dowling, M. B.; Lee, J.-H.; Raghavan, S. R. *Langmuir* **2009**, *25*, 8519.
- (6) Lam, R.; Quaroni, L.; Pedersen, T.; Rogers, M. A. *Soft Matter* **2010**, *6*, 404.
- (7) Zhao, Y.-L.; Stoddart, J. F. *Langmuir* **2009**, *25*, 8442.
- (8) Smith, P. A.; Nordquist, C. D.; Jackson, T. N.; Mayer, T. S.; Martin, B. R.; Mbindyo, J.; Mallouk, T. E. *Appl. Phys. Lett.* **2000**, *77*, 1399.
- (9) Weiss, R. G. Terech, P. In *Molecular Gels Materials with Self-Assembled Fibrillar Networks*; Weiss, R. G.; Terech, P., Eds.; Springer: Dordrecht, The Netherlands, 2007.
- (10) Suzuki, M.; Nakajima, Y.; Yumoto, M.; Kimura, M.; Shirai, H.; Hanabusa, K. *Langmuir* **2003**, *19*, 8622.
- (11) Bot, A.; Agterof, W. G. M. *J. Am. Oil Chem. Soc.* **2006**, *83*, 513.
- (12) Bot, A.; den Adel, R.; Roijers, E. C. *J. Am. Oil Chem. Soc.* **2008**, *85*, 1127.
- (13) Bot, A.; den Adel, R.; Roijers, E. C.; Regkos, C. *Food Biophys.* **2009**, *4*, 266.
- (14) Pernetti, M.; van Malssen, K. F.; Flöter, E.; Bot, A. *Curr. Opin. Colloid Interface Sci.* **2007**, *12*, 221.
- (15) Rogers, M. A. *Food Res. Int.* **2009**, *42*, 747.
- (16) Aro, A.; Jaughiainen, M.; Partanen, R.; Salminen, I.; Mutanen, M. *Am. J. Clin. Nutr.* **1997**, *65*, 1419.
- (17) Roche, H. M. *Proceedings of the Nutrition Society* **2005**, *64*, 23.
- (18) Lin-Vien, D.; Colthup, N. B.; Fateley, W. G.; Grasselli, H. G. In *The Handbook of Infrared and Raman Characteristic Frequencies of Organic Molecules*; Academic Press: New York, 1991.
- (19) den Adel, R.; Heussen, P. C. M.; Bot, A. *J. Phys. Conf. Ser.*, in press.
- (20) Rogers, M. A.; Marangoni, A. G. *Cryst. Growth Des.* **2008**, *8*, 4596.
- (21) Rogers, M. A.; Marangoni, A. G. *Langmuir* **2009**, *25*, 8556.
- (22) Avrami, M. *J. Chem. Phys.* **1939**, *7*, 1103.
- (23) Avrami, M. *J. Chem. Phys.* **1940**, *8*, 212.
- (24) Avrami, M. *J. Chem. Phys.* **1941**, *9*, 177.
- (25) Marangoni, A. G. In *Fat Crystal Networks*; Marangoni, A. G., Eds.; Marcel Dekker: New York, 2005 (Crystallization Kinetics).

JP104101K